View Article Online / Journal Homepage / Table of Contents for this issue

A non-planar organic molecule with non-volatile electrical bistability for nano-scale data storage†

Junping Hu,[ab] Yingfeng Li,[a] Zhuoyu Ji,[ab] Guiyuan Jiang,[c] Lianming Yang,[a] Wenping Hu,[a] Hongjun Gao,[d] Lei Jiang,[a] Yongqiang Wen,[a] Yanlin Song*[a] and Daoben Zhu[a]

Received 5th March 2007, Accepted 4th June 2007
First published as an Advance Article on the web 21st June 2007
DOI: 10.1039/b703332j

A new non-planar organic molecule with electron donor and acceptor capabilities was synthesized for nano-scale data storage. Macroscopic *I–V* characteristics of organic crystalline thin films indicate that the non-planar molecule possesses good electrical bistability. Nano-scale recording dots with an average diameter of 2.5 nm were realized by scanning tunneling microscopy.

Published on 21 June 2007. Downloaded by State University of New York at Stony Brook on 25/10/2014 18:08:47.

Introduction

With the exponential growth of information, high-density data recording media have become the focus of attention.[1] Traditional magnetic materials are widely used today and their density growth is expected to be beyond 100 Gbit in^{-2}.[2] However, when the magnetic recording domain turns as small as nano-scale, problems such as data loss may take place because of the super-paramagnetic effect.[3] With typical optical recording media except for near-field optics, the density of the data stored is restrained by the diffraction limit of the laser beam.[1,4] Herein, exploring new recording materials and advanced recording technologies would be of great significance to satisfy the demand of expansive storage capacity in the future.

Recently, organic materials have received much attention in molecular electronics.[5] Their advantages of designability, low cost and easy manipulation as well as the property of switch or electrical bistability make organic materials attractive. On the other hand, scanning probe microscopies (SPMs),[3,6] including scanning tunneling microscopy (STM),[7] scanning near-field optical microscopy (SNOM)[8] and atomic force microscopy (AFM),[9] have been explored extensively in recent years. It is expected that the combination of organic molecules (one or several molecules as the functional unit) and SPM (manipulation on the nano/atom-scale) will throw light on driving the data storage to ultrahigh density stage. Our group[10–13] has employed a series of organic molecules for information storage with the size of recording marks below 5 nm by STM.

As known, organic molecules serving as a binary system should have two stable states, which indicates that a barrier or threshold between the two states is necessary. Plenty of works have demonstrated that external electric stimulation induces two states that originate from the structural transition,[11] redox,[14] or the charge storage[15,16] mechanism. For instance, Chen *et al.* successfully constructed a polymer/ionic conductor memory device based on electrochemical redox.[14] Yang's group has done several pioneering works in organic/metal devices and pointed out that the memory effect was ascribed to charge storage.[15] Majumdar *et al.* and Pradhan *et al.* have reported works to control the degree of bistability by the concentration of C_{60} or carbon nanotubes in the polymers, and the charge storage mechanism also has been proposed.[16] As for nano-scale data storage, the traditional organic functional films are often made of two components that act as donors and acceptors, respectively.[17] But the problem of inhomogeneity of thin film is difficult to avoid, which would seriously affect the electrical properties. Then, single molecules containing both electron donor (D) and acceptor (A) moieties were used as the binary system. Taking the quality of the crystalline film into account, co-planar molecules were preferred for the application.[11,12] However, the intramolecular and intermolecular charge transfer may interfere with each other, which is related to the quality of the recording media in the aspect of both 'write' and 'read-many-times'. Furthermore, Bandhopadhyay and Pal verified that D–π–A molecules usually have lower on/off current ratio because of the electron conjugation in the molecule, which restrains the usage in high-frequency binary computation.[18] In order to improve the performance of the recording media, in this paper, a strategy is demonstrated to take advantage of both dual-components and sole component; namely, a molecule is designed to contain two separate planar moieties including D and A, respectively, while the two moieties are in a relatively non-planar conformation as an obstacle to avoid the complex interference of intermolecular and intramolecular interaction. As a result, this non-planar configuration would suppress intramolecular coupling for the energy barrier induced by the torsion angle. Meanwhile, the intermolecular charge transfer would be promoted and charge recombination becomes difficult. Hence, the memory would be more stable. Moreover, the non-planar configuration will contribute to a large current ratio of on/off because it perturbs conjugation in the molecular backbone and results

[a]*Key Laboratory of Organic Solids and Laboratory of New Materials, Institute of Chemistry, Chinese Academy of Sciences, Beijing, P. R. China. E-mail: ylsong@iccas.ac.cn; Fax: (+86) 10-82627566*
[b]*Graduate University of Chinese Academy of Sciences, Beijing, P. R. China*
[c]*State Key Laboratory of Heavy Oil Processing, University of Petroleum, Beijing, 102249 P. R. China*
[d]*Nanoscale Physics & Devices, Institute of Physics, Chinese Academy of Sciences, Beijing, 100080 P. R. China*
† Electronic supplementary information (ESI) available: The macroscopic *I–V* characteristics of (ITO/CPMAB/Au) and the long-term response of the 'on' state under an electric field of 1.80 V. See DOI: 10.1039/b703332j

 This journal is © The Royal Society of Chemistry 2007

View Article Online

Published on 21 June 2007. Downloaded by State University of New York at Stony Brook on 25/10/2014 18:08:47.

in a comparatively low conductance state (off).[18] Accordingly, 4-3,4-dicyanophenoxy-4′-dimethyl-aminoazobenzene (CPMAB) was synthesized (see Chart 1). The molecule contains both a D moiety (amino group) and an A moiety (cyano groups), and possesses good thermal stability (without decomposition up to 320 °C). It is noteworthy that an oxygen bridge connects the D and A moieties, which is intended as a barrier between them and presumed to partly contribute to the electrical bistability and the stability. Crystalline films of CPMAB molecules were prepared by vacuum deposition. Macroscopic *I–V* characteristics of the thin films indicate that the non-planar D–A molecules do possess good electrical bistability. Moreover, nano-scale data storage on the thin film was realized by STM. The results suggest that CPMAB may be a promising candidate for non-volatile recording materials.

Experimental

Materials

N,*N*-Dimethylaniline, 4-aminophenol and 4-nitrophthalonitrile from Acros were used without further purification. 4-Hydroxyl-4′-(*N*,*N*-dimethylamino)azobenezene was synthesized from *N*,*N*-dimethylaniline and 4-aminophenol by typical diazotization and coupling reactions.[19] Mp: *ca.* 199–200 °C. ^{1}H NMR ($CDCl_3$, 400 MHz): δ (ppm) 7.84 (d, J = 8.9 Hz, 2H), 7.79 (d, J = 8.8 Hz, 2H), 6.91 (d, J = 8.8 Hz, 2H), 6.76 (d, J = 8.9 Hz, 2H), 4.97 (s, 1H), 3.08 (s, 6H). Anal. calcd for $C_{14}H_{15}N_3O$: C, 69.69; H, 6.27; N, 17.41. Found: C, 69.35; H, 6.13; N, 17.24.

Synthesis of the target compound CPMAB

Under the protection of N_2, dried DMF (20 mL), 4-nitrophthalonitrile (1.44 g, 8.3 mmol), and 4-hydroxyl-4′-(*N*,*N*-dimethylamino)azobenezene (2 g, 8.3 mmol) were in turn added to a flask equipped with a stirrer. Then 5 g of K_2CO_3 were added in portions to the above mixture with stirring over 3 h. Subsequently, the reaction was continued at 25 °C for 8 h. The reaction mixture was then poured slowly into 400 mL of aqueous NaOH (10%, w/w) with stirring. The precipitate was filtered off, washed three times with water and re-crystallized from ethanol to afford a light yellow sheet-like solid of the product CPMAB (2.6 g, yield 85%). Mp: 198 °C. ^{1}H NMR ($CDCl_3$, 400 MHz): δ (ppm) 7.95 (d, J = 8.6 Hz, 2H), 7.91 (d, J = 8.8 Hz, 2H), 7.74 (d, J = 8.8 Hz, 1H), 7.35 (s, 1H), 7.28 (d, J = 8.8 Hz, 1H), 7.16 (d, J = 8.6 Hz, 2H), 6.79 (d, J = 8.8 Hz, 2H), 3.12 (s, 6H). MS (EI, 70 eV) *m*/*z*: 367 [M^+]. Anal. calcd for $C_{22}H_{17}N_5O$: C, 71.92; H, 4.66; N, 19.06. Found: C, 71.64; H, 4.35; N, 19.16.

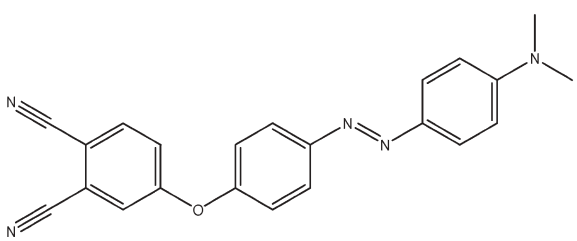

Chart 1 The molecular structure of CPMAB.

Measurements

X-Ray diffraction of the bulk single crystal was measured with a Rigaku RAXIS RAPID imaging plate diffractometer equipped with graphite-monochromated Mo Kα radiation (λ = 0.071073 nm) at 20 °C. The sample was kept in a vacuum oven at 40 °C overnight to eliminate solvent residuals before the measurement. The organic compound CPMAB was deposited onto the substrates under vacuum ($\sim 4 \times 10^{-4}$ Pa) at a rate of 0.1 Å s^{-1} using VPC-260F Vacuum Deposition Equipment (ULVAC), and strict gas elimination prior to deposition. The transmission electron microscope (TEM) image and the selected-area electron diffraction (SAED) pattern were obtained using a Hitachi H-8100 system. The macroscopic *I–V*, *I–t* characteristics were recorded by a Keithley 4200 Semiconductor System and a Micromanipulator 6150 probe station in a clean and shielded box under atmospheric conditions at room temperature. Nano-scale data recording experiments and local *I–V* STS were carried out with a NT-MDT P47 STM under ambient conditions. STM images were acquired continuously in constant current mode, using tips made of tungsten wires (0.3 mm in diameter) by electrochemical etching. Micro-reflection-absorption infrared spectra were measured with a Nicolet Magna IR 750 spectrometer equipped with a microscope (the resolution is 0.125 cm^{-1}, the diameter of the light spot is about 200 μm) and the UV-Vis spectrum was obtained with a Hitachi U-4100 UV-Vis spectrometer. Cyclic voltammogram (CV) was recorded on a Zahner IM6e electrochemical work station using a Pt plate as the working electrode, Pt wire as the counter electrode, and an Ag/Ag^+ electrode as the reference. 0.1 M tetra-*n*-butylammonium hexafluorophosphate (Bu_4NPF_6) dissolved in acetonitrile was employed as the supporting electrolyte.

Results and discussion

Distinguished from organic complex materials,[17] CPMAB contains the donor and acceptor moieties in a single molecule, which could improve the homogeneity of the film. Fig. 1 shows the morphology of the film with a thickness of *ca.* 30 nm by a vacuum deposition method on a Cu grid with amorphous carbon supporting film. The TEM image shows that the organic molecules could form flat uniform films under our experimental conditions. The SAED pattern (Fig. 1, insert) demonstrates the single crystal nature of the thin film. It could be inferred that the CPMAB molecules are stacked in an orderly manner in the thin film by a vacuum deposition method.

To investigate the interaction between the molecules in detail, a red bulk crystal grown from a methylbenzene–dichloromethane (5 : 1) solution was determined by X-ray diffraction‡ after the elimination of solvent residuals. Fig. 2 shows the configuration of CPMAB and the packing diagram

‡ Crystal structure analysis of CPMAB. $C_{22}H_{17}N_5O$, M = 367.41, crystal system: orthorhombic, space group: *Pbca*, a = 7.5300(15) Å, b = 12.173(2) Å, c = 40.996(8) Å, α = 90°, β = 90°, γ = 90°, V = 3757.8(13) $Å^3$, T = 293 K, Z = 8. R (reflections) = 0.0476 (1626), $wR2$ (reflections) = 0.1331 (3010). CCDC reference numbers 624824. For crystallographic data in CIF or other electronic format see DOI: 10.1039/b703332j

View Article Online

Published on 21 June 2007. Downloaded by State University of New York at Stony Brook on 25/10/2014 18:08:47.

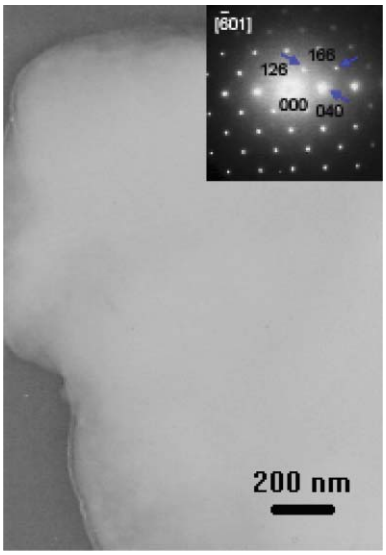

Fig. 1 TEM image and SAED pattern (insert) of the CPMAB film.

of the molecules, which exhibits the relative position of the molecular moieties in the single crystal. As expected, the D and A moieties of CPMAB are in the different planes. By the oxygen bridge, the torsion angle of the D moiety and the A moiety is about 68.7°. C–H···π interaction between C6–H6 of one molecule and the centroid (Cg*) of the C13–C18 ring at $(1 - x, 1 - y, -z)$ has the dimensions of H6···Cg* 2.76 Å and C6–H6···Cg* 152°. This then leads to the formation of centrosymmetric dimers about the inversion centre at (0.5, 0.5, 0). Although the whole molecule is non-planar, the D moiety of a molecule tends to be close and parallel with the A moiety of an adjacent molecule with a distance of about 3.5 Å between them, while the distance between the D group and the A group in the same molecule is larger than 10 Å. Herein, the stack of molecules is favorable for the overlap of intermolecular orbitals in parallel moieties. The result of single crystal X-ray diffraction is in accordance with the SAED indices of thin film shown in Fig. 1.

The stable and ordered crystalline thin film paves the way for the application of the CPMAB molecule in electrical

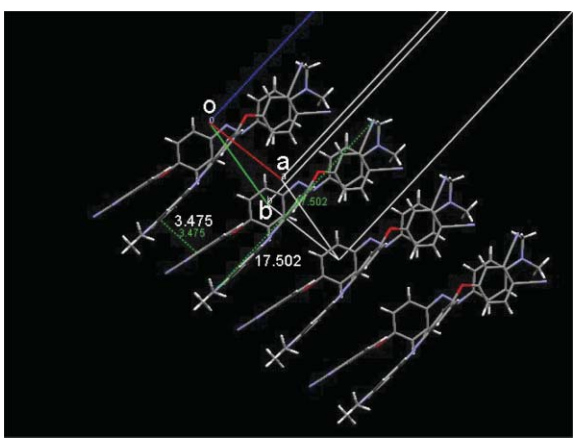

Fig. 2 Viewed down the vectorial (*a*–*b*) direction, it clearly shows that the two planar moieties are approximately parallel with (110) and (−110), respectively.

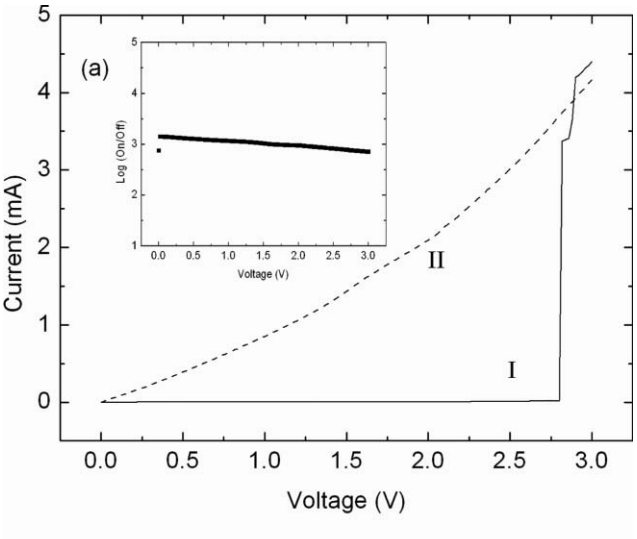

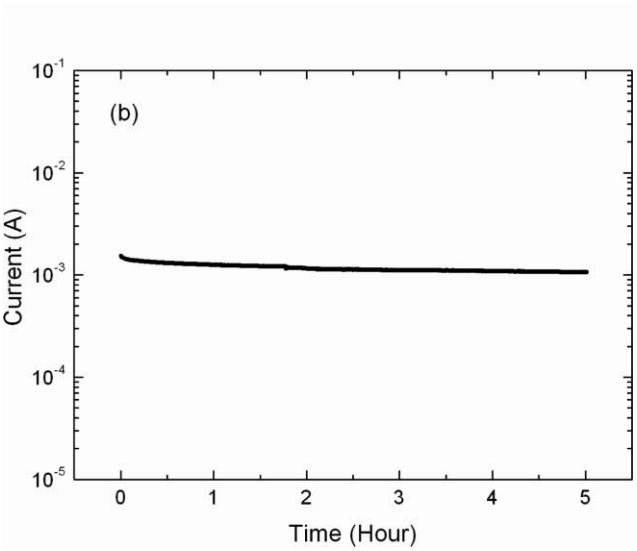

Fig. 3 (a) The macroscopic *I*–*V* characteristics of the CPMAB film by the first scan (curve I, 'off' state) and the second scan (curve II, 'on' state) with an active area 10 × 10 mm^2. The threshold voltage is 2.82 V. Insert shows the logarithm of the 'on' and 'off' state current ratio as a function of the applied voltage. (b) Long-term response of the 'on' state under an electric field of 1.50 V.

devices.[12,13,20] A CPMAB thin film with a thickness of *ca.* 50 nm was deposited on an indium tin oxide (ITO)-coated glass with the sandwich structure ITO/CPMAB(50 nm)/Al(75 nm) and the macroscopic *I*–*V* characteristics were measured with a standard two-terminal system (see the Experimental part). In steps of 0.02 V, the voltage was scanned from 0.00 V to 3.00 V (the bias was applied to the Al electrode). Fig. 3(a) shows *I*–*V* characteristics of the first and the second bias scan, respectively. It can be seen that before the first bias scan, the film shows an insulating behavior ('off' state). The current undergoes a drastic increase when the voltage exceeds the critical value of 2.82 V. In the second bias scan, the current is obviously bigger than in the first scan and the state is termed as the 'on' state. Based on the current values, the conductivity in the 'on' state is about 3 orders of

 This journal is © The Royal Society of Chemistry 2007

View Article Online

Published on 21 June 2007. Downloaded by State University of New York at Stony Brook on 25/10/2014 18:08:47.

magnitude larger than in the 'off' state [insert in Fig. 3(a)]. Furthermore, the film was found to retain the 'on' state non-destructively for more than 5 h under the electric field of 1.50 V [Fig. 3(b)]. In addition, negative bias voltage has also been added to the 'on' state film and it would not turn to the 'off' state even after 5 times scanning from 0.00 to −4.00 V or the application of pulse voltage of −10.00 V for several seconds. Taking the different work function of electrodes into account, an analogous structure of ITO/CPMAB/Au was fabricated, and similar results were obtained (see ESI†). The electrical results indicate that the insulating thin film is switched to a conducting one when the voltage reaches a threshold, and the 'on' state is very stable in case the power is off or even the much larger inversed pulse voltage is applied. Thus, the material has good electrical bistability.

Based on the electrical bistability of the CPMAB thin film, data recording experiments were performed with a P47 STM under ambient conditions using electrochemically etched tungsten tips. CPMAB thin film with a thickness of about 30 nm was deposited on the surface of a freshly cleaved highly oriented pyrolytic graphite (HOPG) substrate. To induce the recording dots, voltage pulses were applied between the STM tip and the HOPG substrate. Fig. 4(a) shows a typical STM image of the recorded pattern on the thin film in a scanning area of 20 × 20 nm^2. The recording dots with an average diameter of 2.5 nm were formed by applying program-controlled voltage pulses of 2.8 V and 6 ms. The pattern was stable during 8 h scanning except for a little thermal drift. Meanwhile, the local conductivity of the dots and other unrecorded places were measured by scanning tunneling spectroscopy (STS). As illustrated in Fig. 4(b), curve I represents the conductivity of the recording dots while curve II shows the state of the unrecorded area. The two conductivity curves differ. The former is in the higher conductivity state and the latter is in the lower one. At half hour intervals, the conductivity of the recording dots and unrecorded area were measured over 8 h and the statistic data were consistent. Compared with the current values shown in Fig. 3(a), they are not in the same order of magnitude for the different active areas and electrodes. However, the trend is obviously consistent; namely, either in macro or micro-scale, the experimental results confirm that the organic thin films are in the low conductivity state before the application of the threshold voltage and in the high conductivity state after that. Therefore, the recording mechanism should be ascribed to the alternation of electrical conductivity before and after the application of the threshold electric field.

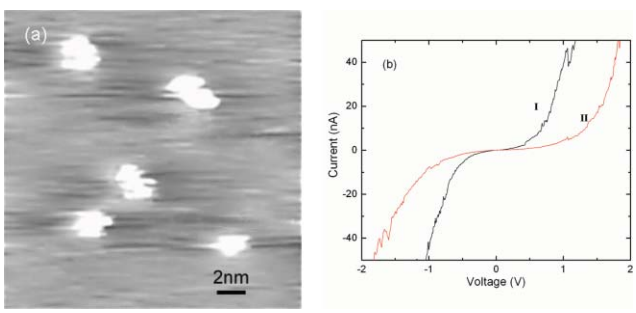

Fig. 4 (a) A typical STM image of the recorded pattern 'z' on the CPMAB thin film in a scanning area of 20 × 20 nm^2. The recording dots, about 2.5 nm in average diameter were formed by applying program-controlled voltage pulses of 2.8 V and 6 ms. The scan condition is V_{bias} = 0.38 V, I_{ref} = 0.043 nA. (b) Local conductivity of the recording dots (Curve I) and unrecorded places (Curve II).

Further investigations were carried out to elucidate the mechanism of the conductivity transition. Micro-reflection-absorption FTIR spectra were recorded before [Fig. 5(a)] and after [Fig. 5(b)] the application of a threshold voltage on the thin film. The stretch vibration of –C≡N exhibits a red-shift (from 2233.4 cm^{-1} to 2231.0 cm^{-1}), which indicates that the cyano group was changed from a neutral to a negatively charged state in the molecule.[12,21] Compared with the literature, the shift of the cyano stretch vibration in FTIR is minor, which suggests a minor change in the electron density of the cyano group. This phenomenon is attributed to the charge delocalization from the cyano group to its connected conjugation moiety. In addtion, the relatively strong vibration at 1602 cm^{-1} might be the result from the lower electron-withdrawing ability of the cyano group towards the benzene ring[22] after the application of voltage.

For organic materials with D and A moieties, intramolecular and intermolecular charge transfer (CT)[23] are two competitive processes.[24] As mentioned above, preventing the positive and negative charges from recombination is significant to the memory devices based on CT.[15] However, the dual operations of intermolecular CT and intramolecular CT might make the contradictive function, *i.e.*, the former would induce charge separation and the latter would lead to charge recombination. In our case, the solution of this problem is suggested to be that the external electric field induces the 'on' state by intermolecular CT, and the non-planar configuration restrains the intramolecular CT to keep the 'on' state stable by preventing the charges from recombination. The appropriate charge delocalization in the separate moieties is suggested to create a stable environment to store the former transferred charges even after the application of a reverse polarity bias.[16] The proposal is validated by the crystal structure of CPMAB, the UV-Vis spectrum, cyclic voltammogram and the

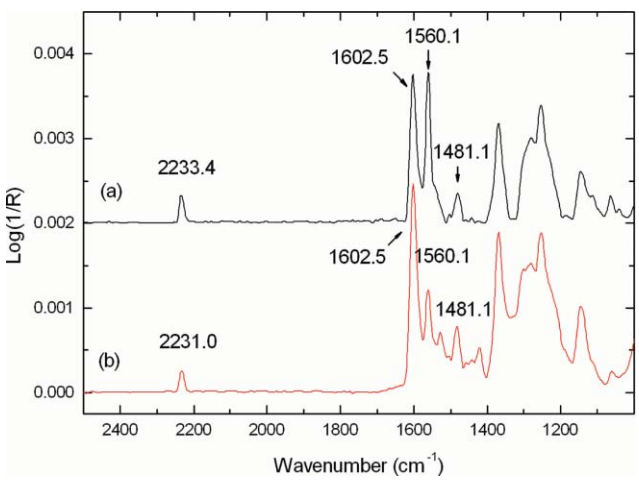

Fig. 5 The micro-reflection-absorption FTIR spectra of the CPMAB thin film before (a) and after (b) the application of a threshold voltage.

View Article Online

Published on 21 June 2007. Downloaded by State University of New York at Stony Brook on 25/10/2014 18:08:47.

theoretical research as follows. On the one hand, the distance between D and A is an important factor to determine the charge transfer. According to the single crystal diffraction data of CPMAB, the distance between the D moiety of one molecule and the A moiety of the adjacent molecule is close to the sum of the van der Waals radii, so electronic coupling between them is dominant and efficient,[25] thus intermolecular CT would play an important role. On the other hand, a theoretical study shows that the intramolecular electron transfer is sensitive to the torsion angle that creates an increasing potential barrier as the dihedral angle varies from co-planar to the perpendicular position.[26] In this case, it is the torsion angle (68.7°) between the two different planar moieties that decreases the conjugation degree of the molecule and keeps stable the charge separation state induced by the intermolecular CT. Additionally, even though the oxygen bridge was considered to transmit the substitution effect in some cases of photophysics,[27] the UV-Vis spectrum of CPMAB (see Fig. 6) shows the ^{1}(n, π*) and ^{1}(π, π*) at comparable energies, indicating the characteristics of 'amino-azobenzenes' rather than those of 'pseudo-stilbenes'.[28] These complementary results confirm that intramolecular CT between the D and A in the same CPMAB molecule is inhibited. The conformation of the two separate planes tends to be in a perpendicular position after the application of the electric field in order to minimize the intramolecular steric repulsion,[26] which might stabilize the intermolecular π–π conjugation further. Herein, for this non-planar D–A configuration, it is reasonable that it would be difficult for charge recombination to take place in the molecule. Cyclic voltammetry (CV) of CPMAB was performed to investigate its electrochemical behavior. As shown in Fig. 7, the onsets of E_{ox} and E_{red} are 0.45 V and −1.66 V *vs* Ag/Ag^+, respectively. The electronic energy levels of the highest occupied molecular orbital (HOMO, −5.16 eV) and the lowest unoccupied molecular orbital (LUMO, −3.05 eV) could be estimated.[29] The enegy gap is about 2.11 eV. That indicates the charge transfer could happen with the threshold voltage. In addition, it should be mentioned that the comparatively high current ratio of on/off can be explained for the reason that the non-planar configuration might make the 'off' state current for the perturbance of electron conjugation in the molecular skeleton low.[18] Therefore, the CPMAB molecule's configuration facilitates the intermolecular CT and excludes the intramolecular CT in the majority, in other words, it is beneficial to keep the recording information stable, which could also be verified by the stability of macroscopic *I–t* characteristics in Fig. 3(b).

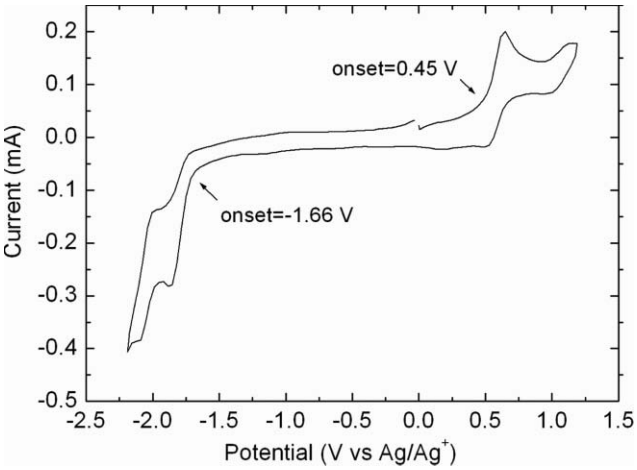

Fig. 7 Cyclic voltammogram of CPMAB in an acetonitrile solution of 0.1 M Bu_4NPF_6 with a potential scan rate of 50 mV s^{-1}.

In order to further confirm the recording mechanism of the CPMAB crystalline thin film, quantum chemical calculations were performed by using the hybrid Hartree–Fock/density-functional-theory (HF/DFT) method of B3LYP[30] with the 6-31G* basis set.[31] Fig. 8 shows HOMO and LUMO of the CPMAB molecule. It is obvious that the amino moiety contributes more to HOMO than to the LUMO while the cyano moiety does the reverse. The configuration of the two separate planar moieties in the molecule tends to a perpendicular position, which is consistent with the results from X-ray diffraction. Although the energy levels from the calculation do not match exactly with the results of CV measurements regardless of a strong local field,[18] the matching molecular orbitals make it reasonable that the charge transfers from the

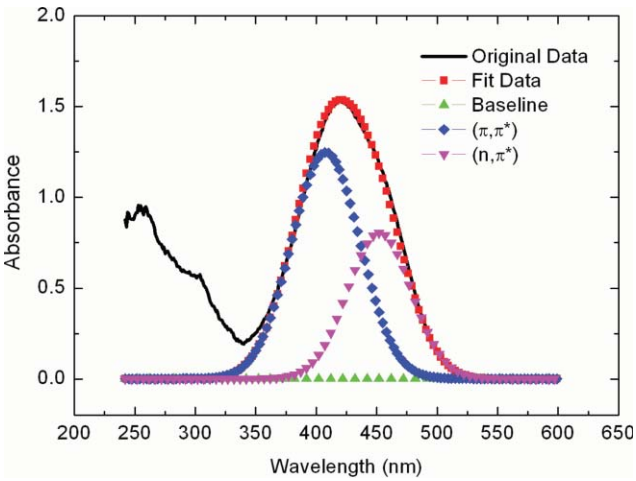

Fig. 6 UV-Vis spectrum of CPMAB in CH_2Cl_2 (~6.0 × 10^{-5} mol L^{-1}).

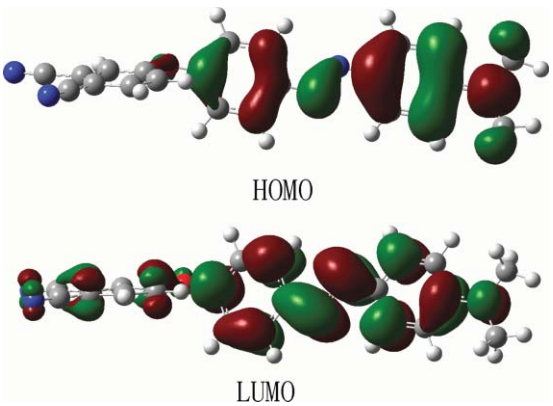

Fig. 8 The HOMO and LUMO molecular orbitals of CPMAB calculated by the HF/DFT method of B3LYP with the 6-31G* basis set.

 This journal is © The Royal Society of Chemistry 2007

View Article Online

Published on 21 June 2007. Downloaded by State University of New York at Stony Brook on 25/10/2014 18:08:47.

amino moiety of one molecule to the cyano moiety of the adjacent molecule under the application of the electric field; and the non-planar configuration does much to prohibit the charge recombination. Additionally, the theoretical calculation also shows that the oxygen atom contributes little to the molecular orbitals, which would hardly influence the charge character of the D and A.

Conclusions

In summary, in order to combine the advantages of dual-component and sole component donor–acceptor materials, a new non-planar organic compound with separate electron donor and acceptor moieties was synthesized, and its homogeneous crystalline films were prepared by vacuum deposition. The thin film possesses good electrical bistability with high current ratio of 'on' and 'off', and the 'on' state is very stable in the long-term response. Nano-scale recording marks were successfully realized on a thin film by STM and the recording mechanism was discussed. Electrical bistability was ascribed to intermolecular charge transfer and the non-planar configuration benefits stable data storage as it can exclude the interference of intramolecular charge transfer. The results indicate that CPMAB is a promising candidate for nano-scale recording materials. Further design of such non-planar molecules and fine control of the charge transfer by the length and rigidty of the linker between the D and A moieties are undergoing, which might provide new strategies for developping novel functional materials for nano-scale data storage.

Acknowledgements

The authors thank for financial support, the NSFC (Grant Nos. 50625312, 60601027, U0634004 and 20421101), the 973 Program (No.2006CB806200, 2006CB932100) and the Chinese Academy of Sciences. The authors also thank the reviewers for the constructive comments and suggestions that helped improve the manuscript greatly.

References

1 H. Mustroph, M. Stollenwerk and V. Bressau, *Angew. Chem., Int. Ed.*, 2006, **45**, 2016.
2 D. Weller and A. Moser, *IEEE Trans. Magn.*, 1999, **35**, 4423; D. Weller, A. Moser, L. Folks, M. E. Best, W. Lee, M. F. Toney, M. Schwickert, J. U. Thiele and M. F. Doerner, *IEEE Trans. Magn.*, 2000, **36**, 10.
3 M. I. Lutwyche, M. Despont, U. Drechsler, U. Dürig, W. Häberle, H. Rothuizen, R. Stutz, R. Widmer, G. K. Binnig and P. Vettiger, *Appl. Phys. Lett.*, 2000, **77**, 3299.
4 B. D. Terris, H. J. Marmin and D. Rugar, *Appl. Phys. Lett.*, 1996, **68**, 141–143.
5 J. M. Tour, *Acc. Chem. Res.*, 2000, **33**, 791–804; A. R. Pease, J. O. Jeppesen, J. F. Stoddart, Y. Luo, C. P. Collier and J. R. Heath, *Acc. Chem. Res.*, 2001, **34**, 433.
6 S. Hosaka, S. Hosoki, T. Hasegawa, H. Koyanagi, T. Shintani and M. Miyamoto, *J. Vac. Sci. Technol., B*, 1995, **13**, 2813.
7 A. Sato and Y. Tsukamoto, *Nature*, 1993, **363**, 431; H. L. Peng, C. B. Ran, X. C. Yu, R. Zhang and Z. F. Liu, *Adv. Mater.*, 2005, **17**, 459.
8 S. Hosaka, T. Shintani, M. Miyamoto, A. Kikukawa, A. Hirotsune, M. Terao, M. Yoshida, K. Fujita and S. J. Kämmer, *J. Appl. Phys.*, 1996, **79**, 8082; A. Vertikov, M. Kuball, A. V. Nurmikko, Y. Chen and S. Y. Wang, *Appl. Phys. Lett.*, 1998, **72**, 2645.
9 G. Binnig, M. Despond, U. Drechsler, W. Häberle, M. Lutwyche, P. Vettiger, H. J. Mamin, B. W. Chui and T. W. Kenny, *Appl. Phys. Lett.*, 1999, **74**, 1329; K. Yano and T. Ikeda, *Appl. Phys. Lett.*, 2002, **80**, 1067.
10 L. P. Ma, Y. L. Song, H. J. Gao, W. B. Zhao, H. Y. Chen, Z. Q. Xue and S. J. Pang, *Appl. Phys. Lett.*, 1996, **69**, 3752.
11 D. X. Shi, Y. L. Song, H. X. Zhang, P. Jiang, S. T. He, S. S. Xie, S. J. Pang and H. J. Gao, *Appl. Phys. Lett.*, 2000, **77**, 3203; D. X. Shi, Y. L. Song, D. B. Zhu, H. X. Zhang, P. Jiang, S. S. Xie, S. J. Pang and H. J. Gao, *Adv. Mater.*, 2001, **13**, 1103; M. Feng, X. F. Guo, X. Lin, X. B. He, W. Ji, S. X. Du, D. Q. Zhang, D. B. Zhu and H. J. Gao, *J. Am. Chem. Soc.*, 2005, **127**, 15338.
12 J. C. Li, Z. Q. Xue, K. Z. Wang, Z. M. Wang, C. H. Yan, Y. L. Song, L. Jiang and D. B. Zhu, *J. Phys. Chem. B*, 2004, **108**, 19348.
13 H. M. Wu, Y. L. Song, S. X. Du, H. W. Liu, H. J. Gao, L. Jiang and D. B. Zhu, *Adv. Mater.*, 2003, **15**, 1925; Y. Q. Wen, Y. L. Song, G. Y. Jiang, D. B. Zhao, K. L. Ding, W. F. Yuan, X. Lin, H. J. Gao, L. Jiang and D. B. Zhu, *Adv. Mater.*, 2004, **16**, 2018; G. Y. Jiang, T. Michinobu, W. F. Yuan, M. Feng, Y. Q. Wen, S. X. Du, H. J. Gao, L. Jiang, Y. L. Song, F. Diederich and D. B. Zhu, *Adv. Mater.*, 2005, **17**, 2170; Y. Q. Wen, J. X. Wang, J. P. Hu, L. Jiang, H. J. Gao, Y. L. Song and D. B. Zhu, *Adv. Mater.*, 2006, **18**, 1983.
14 Q. X. Lai, Z. H. Zhu and Y. Chen, *Appl. Phys. Lett.*, 2006, **88**, 133515.
15 L. P. Ma, J. Liu and Y. Yang, *Appl. Phys. Lett.*, 2002, **6**, 2997; J. Y. Ouyang, C. W. Chu, C. R. Szmanda, L. P. Ma and Y. Yang, *Nat. Mater.*, 2004, **3**, 918; C. W. Chu, J. Ouyang, J. Tseng and Y. Yang, *Adv. Mater.*, 2005, **17**, 1440; Y. Yang, J. Ouyang, L. Ma, R. J. Tseng and C. Chu, *Adv. Funct. Mater.*, 2006, **16**, 1001.
16 H. S. Majumdar, J. K. Baral, R. Österbacka, O. Ikkala and H. Stubb, *Org. Electron.*, 2005, **6**, 188; B. Pradhan, S. K. Batabyal and A. J. Pal, *J. Phys. Chem. B*, 2006, **110**, 8274.
17 J. Gong and Y. Osada, *Appl. Phys. Lett.*, 1992, **61**, 2787; H. J. Gao, K. Sohlberg, Z. Q. Xue, H. Y. Chen, S. M. Hou, L. P. Ma, X. W. Fang, S. J. Pang and S. J. Pennycook, *Phys. Rev. Lett.*, 2000, **84**, 1780.
18 A. Bandhopadhyay and A. J. Pal, *J. Phys. Chem. B*, 2003, **107**, 2531.
19 Y. J. Cui, M. Q. Wang, L. J. Chen and G. D. Qian, *Dyes Pigm.*, 2005, **65**, 61; H. Zollinger, *Color Chemistry*, WileyVCH press, Zurich, 3rd edn, 2003, p. 165.
20 G. Y. Jiang, Y. L. Song, Y. Q. Wen, W. F. Yuan, H. M. Wu, Z. Yang, A. D. Xia, M. Feng, S. X. Du, H. J. Gao, L. Jiang and D. B. Zhu, *ChemPhysChem*, 2005, **6**, 1478.
21 J. S. Chappell, A. N. Bloch, W. A. Bryden, M. Maxfield, T. O. Poehler and D. O. Cowan, *J. Am. Chem. Soc.*, 1981, **103**, 2442; K. Z. Wang, Z. Q. Xue, M. Ouyang, D. W. Wang, H. X. Zhang and C. H. Huang, *Chem. Phys. Lett.*, 1995, **243**, 217.
22 L. R. Wen, M. Li and G. L. Zhao, *Chin. J. Spectrosc. Lab.*, 2004, **21**, 244.
23 E. Bosch, R. Radford and C. L. Barnes, *Org. Lett.*, 2001, **3**, 881; S. V. Lindeman, J. Hecht and J. K. Kochi, *J. Am. Chem. Soc.*, 2003, **125**, 11597; S. Sumalekshmy and K. R. Gopidas, *J. Phys. Chem. B*, 2004, **108**, 3705.
24 E. H. A. Beckers, S. C. J. Meskers, A. P. H. J. Schenning, Z. J. Chen, F. Würthner, P. Marsal, D. Beljonne, J. Cornil and R. A. J. Janssen, *J. Am. Chem. Soc.*, 2006, **128**, 649.
25 M. N. Paddon-Row, *Acc. Chem. Res.*, 1994, **27**, 18; R. Hoffmann, A. Imamura and W. J. Hehre, *J. Am. Chem. Soc.*, 1968, **90**, 1499; M. D. Curtis, J. Cao and J. W. Kampf, *J. Am. Chem. Soc.*, 2004, **126**, 4318.
26 I. Cacelli, A. Feretti, M. Girlanda and M. Macucci, *Chem. Phys.*, 2006, **320**, 84.
27 W. Huang, X. Zhang, L. H. Ma, C. J. Wang and Y. B. Jiang, *Chem. Phys. Lett.*, 2002, **352**, 401.
28 H. Rau, in *Photochemistry and Photophysics*, ed. J. K. Rabek, CRC Press, Boca Raton, FL, 1990, vol. 2, p 119; Z. Sekkat and W. Knoll, *Photoreactive Organic Thin Films*, Elsevier Science, USA, 2002, pp. 6–7.
29 Q. J. Sun, H. Q. Wang, C. H. Yang and Y. F. Li, *J. Mater. Chem.*, 2003, **13**, 800.
30 C. Lee, W. Yang and R. G. Parr, *Phys. Rev. B*, 1988, **37**, 785.
31 W. J. Hehre, L. Radom, P. v. R. Schleyer and J. A. Pople, *Ab Initio Molecular Orbital Theory*, Wiley-Interscience, New York, 1986.